

**ADVANCES IN  
FOREST FIRE RESEARCH  
2018**

EDITED BY

**DOMINGOS XAVIER VIEGAS**  
ADAI/CEIF, UNIVERSITY OF COIMBRA, PORTUGAL

# Lattice Boltzmann Method for Flow through Vegetation

Hayri Sezer<sup>1,2</sup>; Albert Simeoni<sup>1\*</sup>

<sup>1</sup>Worcester Polytechnic Institute, Worcester, MA, 01609, USA {[asimeoni@wpi.edu](mailto:asimeoni@wpi.edu)\*

<sup>2</sup>School of Engineering and Technology, Western Carolina University, USA

## Abstract

Recently wildland/forest fires have dramatic impact on the environment and society. Therefore, it is vital to understand wildland/forest fires spread dynamics to prevent its hazardous effects on society and environment. Models based on Computational Fluid Dynamics (CFD) have been developed and improved to investigate the dynamics of the wildland/forest fires. Even for CFD based physical models, a robust understanding of the processes (i.e. drag, convective heat transfer and radiation) driving fire spread is missing for small scale. The present study focuses on obtaining drag coefficient for the complex vegetation structures in small scales by using Lattice Boltzmann method (LBM). Ultimately, the drag coefficient can be used in detailed wildland/forest fire spread models to analyze the physical mechanisms driving the fire spread in vegetation. The Lattice Boltzmann (LBM) is a relatively new numerical approach for solving Navier-Stokes equations. LBM has advantages such as simplicity, efficiency, easy treatment of boundary conditions, easy parallelization in simulating fluid flow and heat transfer. The developed model is validated with experiment for a cylinder in cross flow in the literature. The results show that LBM method can be used for the flow in complex distribution of vegetation.

**Keywords:** LBM, complex fuels, drag coefficient, wildland fire

## 1. Introduction

Wildland fires can be beneficial and catastrophic for the environment and society. Prescribed fires can have a positive impact on the environment including reducing grass, brushes and trees. However, wildland fires happening in the wrong place at the wrong time can have a dramatic impact on lives, property, whole communities, and natural and cultural resources (U.S. Forest Service, 2018). Therefore, it is vital to better understand the dynamics of wildfire spread to help manage forests, other ecosystems and help protect human life, property, and activities.

Fire spread in heterogenous fuels is a result of the interaction between the solid and gas phases, as well as radiative heat transfer between phases. Models based on computational fluid dynamics (CFD) have been developed to address the complicated combustion processes involved in wildland fires (Larini, M., *et al.*, 1988; J.L. Dupuy *et al.*, 2005; Zhou, X. *et al.*, 2007; Mell, W. *et al.*, 2009). However, the CFD models apply strong and unverified assumption to resolve some small-scale processes, including drag forces and convective heat transfer. For instance, the drag coefficient is an input parameter in CFD based physical models that is based on a single cylinder in a cross-flow (Mell, W., *et al.*, 2009). In this study, an attempt has been made to resolve sub-grid scale processes involved in fire dynamics by using an in-house developed two-dimensional Navier-Stokes solver based on the Lattice Boltzmann Method (LBM).

Recently, the LBM has become an alternative numerical method for computing fluid flow and heat transfer. The LBM is particularly successful in applications including interfacial dynamics and complex boundaries because of its boundary condition implementation. The basic idea behind the LBM is to build simplified Boltzmann equations that relate the main physics of the microscopic processes (particle distribution and equilibrium distribution functions) such that the macroscopic process averaged properties including density, temperature, velocity and pressure obey the desired governing equations (i.e. Navier Stokes and scalar transport equations) (Chen, S. *et al.*, 1998).

In the present study, the drag coefficient at grid scale is directly calculated through the LBM for different configurations of cylinders in a cross flow.

## 2. Lattice Boltzmann method

The numerical model was developed for non-isothermal flows based on the LBM. The LBM uses a simple boundary condition scheme that can easily handle the flow in complex boundaries similar to vegetation (A.A. Mohamad, 2011). The current model is able to solve the momentum and energy equations for rigid bodies. The LBM method is based on the Boltzmann transport equation for a dynamic system. The Boltzmann equation for a system without an external force is written as (A.A. Mohamad, 2011),

$$\frac{\partial f}{\partial t} + c\nabla f = -\frac{1}{\tau}(f - f^{eq}) \quad (1)$$

Where  $f$ ,  $f^{eq}$  and  $\tau$  are the particle distribution function, particle equilibrium function and relaxation time, respectively. Equation 1 is similar to the advection equation with a source term and it can be solved by a finite difference method. However, in LBM, Eq. 1 is solved by a streaming and a collision step (Wang, J., *et al.*, 2007).

### 1.1. Drag Coefficient

The drag coefficient can be calculated from the estimation of the total drag force that is acting on an obstacle or from the pressure drop that is induced by the obstacle in the flow. The drag coefficient is defined as;

$$\text{Drag force; } C_D = \frac{F_x}{\frac{1}{2}\rho U^2 D} \quad (2)$$

$$\text{Pressure drop; } C_D = \frac{P_{in} - P_{out}}{\frac{1}{2}\rho U^2}$$

The following equation was used to estimate the total force from a fluid acting on an obstacle (Mei, R., *et al.*, 2002):

$$F = \sum_{x_b} \sum_{k \neq 0} c_k [f_k(x_b, t) + f_k^-(x_b + c_k^- \Delta t, t)] \times [1 - (x_b + c_k^- \Delta t)] \quad (3)$$

Where  $x_b$  is the boundary nodes of the obstacle and  $c_k^-$  is the opposite direction of  $c_k$ .

### 2.1. Verification and Validation

A flow over an obstacle has many practical applications in buildings, bridges, heat exchangers and wildland fires. The flow, under certain conditions causes pressure vortices downstream of an obstacle and forms vortex shedding depending on the Reynolds number. To capture this dynamic fluctuation of the flow with the LBM, a square channel shown in Fig.1 is selected, with a circular cylinder with a blockage ratio of 1 to 8 located in its center. The geometry, boundary conditions, and grid used in the simulation are shown in Fig. 1. The curvature boundary of the cylinder is zoomed out to depict the boundary nodes, solid nodes and the fluid nodes used in the simulations. On-grid bounce-back boundary conditions are used for the obstacle as well as the top and the bottom walls (Gallivan, M.A., *et al.*, 1997). Zou-He velocity and pressure boundary conditions (Zou, Q. and He, X., 1997) are implemented at the inlet and the outlet (see Figure 1). The simulations with  $Re = 20$  and  $40$  were carried out and the flow pattern is in good agreement with prior results from laboratory experiments (Bao, Y.B. and Meskas, J., 2011) (see Figure 2).

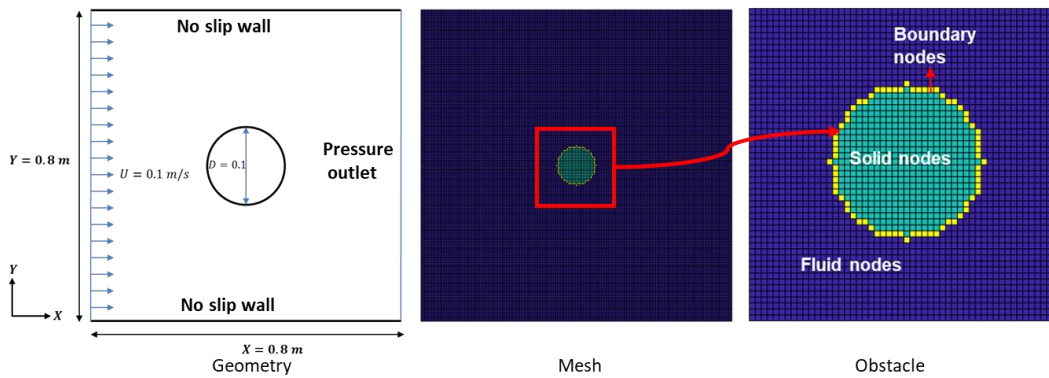


Figure 1 - Representation of geometry, mesh and obstacle used in the drag coefficient calculation

A pair of fixed symmetric vortices is generated in the wake of the cylinder in the simulation with LBM and the results match the laboratory image by Bao et al (Bao, Y.B. and Meskas, J., 2011), as seen in Fig. 2.

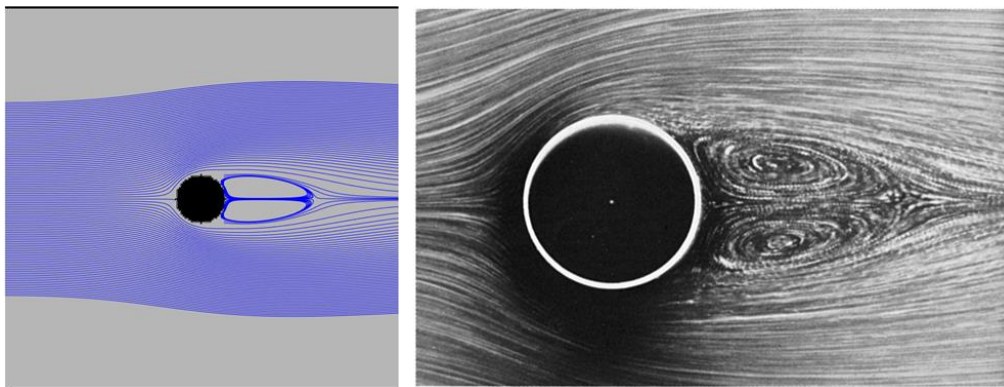


Figure 2 - A fixed pair of vortices: simulation vs experiment (Bao et al., 2011) (Bao, Y.B. and Meskas, J., 2011)

Table 1 - Drag coefficient at different Reynolds number

	Re = 20	Re = 40
Tritton experiment <sup>1</sup>	2.22	1.48
Current study	2.3	1.56
<sup>1</sup> (Tritton D., 1959)		

Drag coefficients with  $Re = 20$  and  $40$ , calculated by the present model and obtain from the literature are listed in Table 1. As it can be seen, the current model agrees reasonably well with the experimental measurements by Tritton. (Tritton D., 1959).

### 3. Results and discussion

The calculation of the vegetation drag coefficient is required for the modeling of fire spread in wildlands, but also for the flow in river beds and on flood plains (Kim, S.J. and Stoesser, T., 2011; Fischer-Antze, T., *et al.*, 2001). The drag exerted on the flow by vegetation changes with the plant shape, rigidity, and with the spatial distribution of vegetation. In many experimental studies of flow through vegetation, the cylinder analogy is used. For example, vegetation can be represented as a bunch of rigid circular cylinders (Kim, S.J. and Stoesser, T., 2011). In the present study, the drag coefficient is directly calculated for simplified geometries that can represent a rigid vegetation such

as, single cylinder, inline and staggered arrays of cylinders as well as randomly distributed cylinders in a cross flow.

### 3.1. Single Cylinder

The drag coefficient for a cylindrical obstacle depends on the behavior of the fluid around the cylinder. For example, depending on the Reynolds number, the flow pattern near the cylinder can vary significantly. For higher Reynolds number (i.e.  $Re_D > 40$ ), an unsteady wake flow occurs, the characteristic of which depends on the Reynolds number. In the following simulations the Reynolds number is defined as follow:

$$Re_D = \frac{U_\infty D}{\nu} \quad (4)$$

Where  $\nu$  is the fluid kinematic viscosity,  $U_\infty$  is the upstream velocity, and  $D$  is the cylinder diameter.

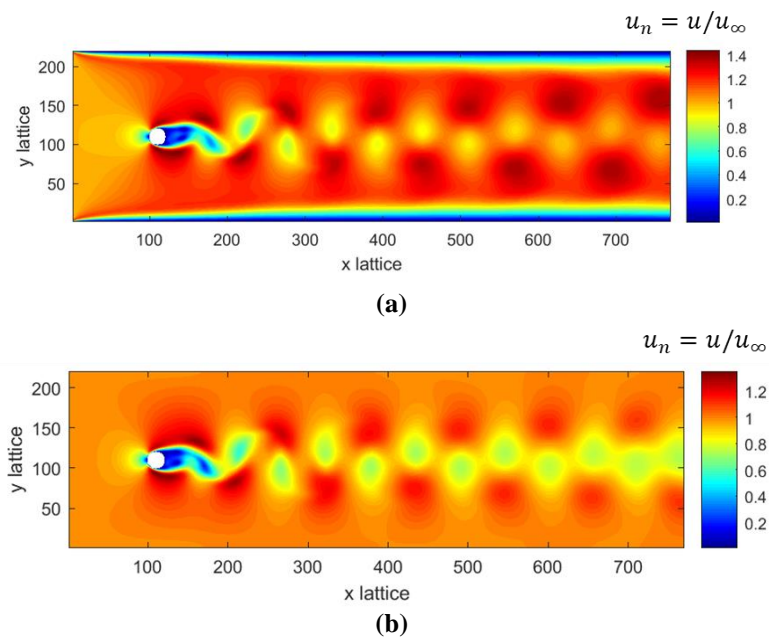


Figure 3 - Contours of velocity magnitude for flow around a cylindrical object at  $Re_D = 100$ . (a) no-slip wall (b) periodic boundary conditions at top and bottom walls.

For a single cylinder, simulations have been carried out at  $Re_D = 100$ , with no-slip and periodic boundary conditions at the walls to estimate the effect of different wall boundary condition on estimation of the drag coefficient. A uniform velocity was set at the inlet and a pressure outlet boundary condition was implemented at the outlet, as shown in Fig. 1 (geometry). Contours of the velocity magnitude shown in Fig. 4 were generated at the steady state flow for the no-slip and periodic boundary conditions. The vortex shedding can be observed downstream of the cylinders. The calculated drag coefficient for both cases and the literature values are listed in Table 2. As shown in Table 2, the current study agrees well with the literature for the no-slip wall boundary condition. However, there is a deviation when a periodic boundary condition is used. The deviation is introduced by the friction presence of a rigid wall at the boundaries. In order to remove the effect of no-slip wall condition, in the following simulations, periodic boundary condition is implemented at the walls.

Table 2- Drag coefficient at  $Re_D = 100$  for a single cylinder.

2-D simulation	Drag coefficient at $Re_D = 100$
Braza et al. (1986) <sup>1</sup>	1.34
Kjellgren (1997) <sup>2</sup>	1.34
Su and Kang (1999) <sup>3</sup>	1.34
Lam et al. (2008) <sup>4</sup>	1.36
Current study, LBM (no-slip)	1.34
Current study, LBM (periodic)	1.25

<sup>1</sup>(Braza, M., Chassaing, P., Ha Minh, H., 1986), <sup>2</sup>(Kjellgren, P., 1997), <sup>3</sup>(Su, M., Kang, Q., 1999), <sup>4</sup>(Lam, K., et al., 2008)

### 3.2. Inline and staggered arrays of cylinders

The drag coefficient of cylinders in a cross flow is relevant to different industrial applications, including heat exchangers, boilers, and air conditioners. The cylinders in industrial applications are usually either aligned or staggered relative to the stream-wise fluid velocity. Cylinders in a cross flow can also represent an idealized rigid vegetation. Fluid flow through circular cylinders is dictated by the boundary layer separation and wake interaction, which in-turn affect the drag coefficient. Therefore, cylinders in different configurations are used to calculate the drag coefficient. The LBM based N-S solver is used to simulate the flow through inline and staggered array of the cylinders at Reynolds number of 100. The cylinders in the inline and staggered configurations are equivalent. The top and bottom walls are 10 cylinder diameters away from the vegetation area. Figure 4 shows the contours of velocity magnitude the steady state flow for inline and staggered arrays of cylinders in a cross flow. It can be seen that the flow patterns for the inline and staggered arrays of cylinder are significantly different from each other. However, the maximum normalized velocity is similar. The drag solid fraction of the inline and staggered array of cylinders are 0.14 and 0.11 respectively, whereas, the drag coefficients are 0.57 and 0.83. The solid fraction of the vegetation is the ratio of the solid cylinder's area to the smallest rectangular area that encompass the cylinders. As it seen in Fig. 4, the flow pattern of the inline array and staggered array are significantly different because of the cylinder's arrangement. Therefore, the drag coefficients are different for both cases even though the solid fraction is not significantly different. The LBM is able to predict the fluid flow behavior through idealized vegetation configurations such as inline and staggered arrangements. The comparison of the inline, staggered and randomly distributed cylinders are given in the subsequent sections.

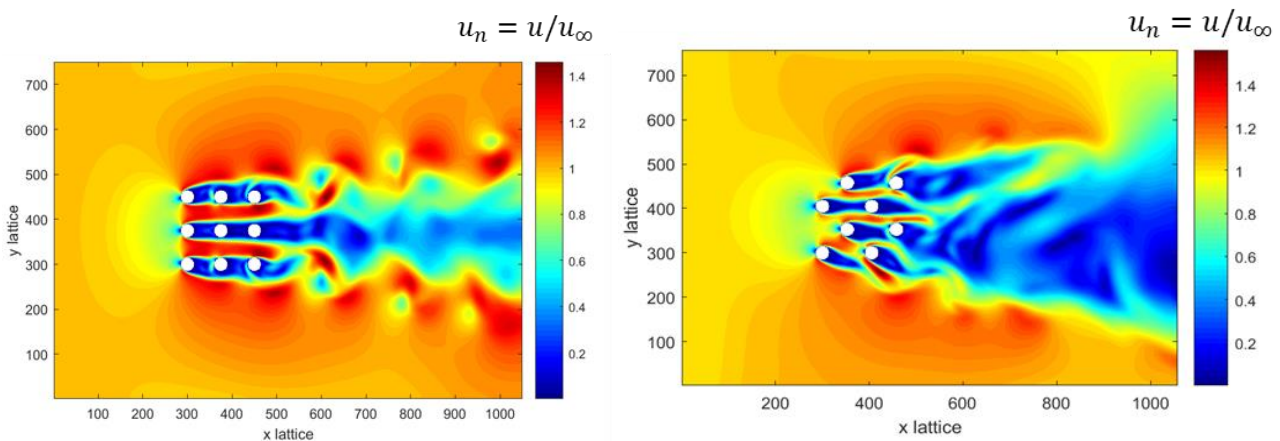


Figure 4 - Contours of velocity magnitude for a flow through an array of cylinders at  $Re_D = 100$ . (top) inline, (bottom) staggered

### 3.3. Randomly distributed cylinders

A random distribution may better represent vegetation structures in their natural state than the inline and staggered arrays of cylinders. Therefore, the developed LBM code was used to calculate the drag

coefficient for randomly distributed cylinders in a cross flow for different solid fractions and numbers of cylinders. Figure 5 shows the contours of the velocity magnitude at steady state flow for different randomly distributed cylinders in a cross flow. As it can be seen, the flow pattern is different for both cases and therefore, the drag exerted by randomly distributed rigid circular cylinders is significantly different for two densities of 0.11 and 0.093. The corresponding drag coefficients are 1.37 and 2.7 respectively.

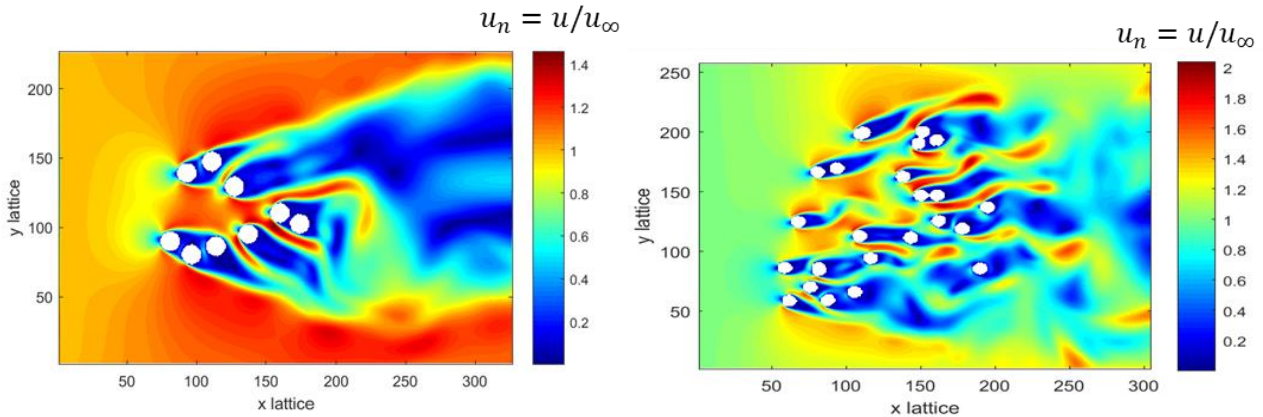


Figure 5 - Contours of velocity magnitude for a flow through randomly distributed cylinders at  $Re_D = 100$ . (top) bulk density,  $\phi = 0.11$  (bottom)  $\phi = 0.093$

### 3.4. Drag coefficient comparison

Additional simulations are performed to analyze the drag coefficient for different configurations as well as vegetation solid fraction and compare the results with the available literature. Table 3 summarizes the numerical simulations and calculated drag coefficients. For the time being, the numerical simulations are carried out at a relatively low Reynolds number of 100 because of the current limitations of the turbulence model in the LBM.

Table 3 - Summary of the numerical simulations of drag coefficient calculation

solid fraction	$Re_D$	B. C.	$C_D$	Shape	Configuration	study
0.14	100	periodic	0.57	cylinder	inline	LBM
0.50	100	periodic	0.66	cylinder	inline	LBM
0.26	100	periodic	0.68	cylinder	inline	LBM
0.20	100	periodic	0.74	cylinder	inline	LBM
0.24	100	wall	0.775	cylinder	inline	(Lam, K., <i>et al.</i> , 2008)
0.10	100	periodic	0.59	cylinder	inline	LBM
0.21	100	periodic	0.5	cylinder	inline	LBM
0.21	100	wall	0.64	cylinder	inline	LBM
0.078	100	wall	1.5	cylinder	inline	LBM
0.078	100	periodic	1.41	cylinder	inline	LBM
0.11	100	periodic	0.83	cylinder	staggered	LBM
0.2	100	periodic	0.44	cylinder	staggered	LBM
0.087	695	wall	2.02	cylinder	staggered	(Kim, S.J. and Stoesser, T., 2011)
0.11	100	periodic	1.37	cylinder	random	LBM
0.065	100	periodic	1.95	cylinder	random	LBM
0.093	100	periodic	2.7	cylinder	random	LBM
0.04	100	periodic	2.7	cylinder	random	LBM
0.11	100	periodic	2.3	cylinder	random	LBM
0.16	100	periodic	2.19	cylinder	random	LBM
0.15	193	wall	3.03	cylinder	random	(Tanino, Y., and H. M. Nepf, 2008)
0.15	263	wall	2.86	cylinder	random	(Tanino, Y., and H. M. Nepf, 2008)

As it can be seen in Table 3, the simulated results are in the range of the experimental results by Kim et al. (Kim, S.J. and Stoesser, T., 2011) and Tanino et al. (Tanino, Y., and H. M. Nepf, 2008) . However, it should be noted here that, the experimental results by Kim et al and Tanino are performed at higher Reynolds numbers. In the LBM method, fluid flow with high Reynolds number can be utilized by implementing a Multiple Relaxation Time scheme (MRT) and a Smogrosky LES-LBM model. Also, the current LBM model can be used to simulate higher Reynolds number flows with a fine grid resolution. However, a fine grid resolution simulation increases the computational cost. In future works, An MRT-LBM scheme will be developed to simulate the fluid flow at higher Reynolds numbers. In addition, a Smogrosky-LES model will be tested for drag coefficient calculations of turbulent fluid flows.

#### **4. Conclusion**

A computational model based on the Lattice Boltzmann method (LBM) has been developed to predict the drag coefficient for idealized vegetation structure including inline, staggered and randomly distributed configurations. The drag coefficient for a single cylinder in the cross flow has been calculated and validated with available experiments at relatively low Reynolds numbers of 20, 40 and 100. Additional simulations, with different cylinder configurations in cross flow, were performed at a Reynolds number of 100. The LBM simulations are compared with experimental and numerical studies in the literature. The LBM based simulations closely match with the numerical simulations presented in the literature. And the simulated results match with the experimental measurements reasonably well. The differences between the experimental measurements and the simulations are due to the different flow conditions i.e. higher Reynolds number flow used in the experimental work, the number of the cylinders used in the staggered and inline arrays, and the solid fractions. The model will be used to calculate the convective heat transfer and drag coefficient for complex geometries representative of vegetation structure. The prediction of this model can be used in WFDS or other CFD models to improve the modeling of vegetation, through a more accurate estimation of the drag coefficient.

#### **5. References**

- A.A. Mohamad. (2011). Lattice Boltzmann method: fundamentals and engineering applications with computer codes. London: Springer-Verlag.
- Bao, Y.B. and Meskas, J. (2011). Lattice Boltzmann method for fluid simulations. . New York: Department of Mathematics, Courant Institute of Mathematical Sciences, New York University.
- Braza, M., Chassaing, P., Ha Minh, H. (1986). Numerical study and physical analysis of the pressure and velocity fields in the near wake of a circular cylinder. *Journal of Fluid Mechanics* , 165, 79–130.
- Chen, S. and Doolen, G.D. (1998). Lattice Boltzmann method for fluid flows. *Annual review of fluid mechanics*, 30(1), 329-364.
- Fischer-Antze, T., Stoesser, T., Bates, P. and Olsen, N.R.B. (2001). 3D numerical modelling of open-channel flow with submerged vegetation. *Journal of Hydraulic Research*, 39(3), 303-310.
- Gallivan, M.A., Noble, D.R., Georgiadis, J.G. and Buckius, R.O. (1997). An evaluation of the bounce-back boundary condition for lattice Boltzmann simulations. *International Journal for Numerical Methods in Fluids*, 25(3), 249-263.
- J.L. Dupuy, D. Morvan. (2005). Numerical study of a crown fire spreading toward a fuel break using a multiphase physical model. *International Journal of Wildland Fire*, 14(2), 141-151.
- Kim, S.J. and Stoesser, T. (2011). Closure modeling and direct simulation of vegetation drag in flow through emergent vegetation. *Water Resources Research*, 47(10).

- Lam, K., Gong, W.Q. and So, R.M.C. (2008). Numerical simulation of cross-flow around four cylinders in an in-line square configuration. *Journal of Fluids and Structures*, 24(1), 34-57.
- Larini, M., Giroud, F., Porterie, B. and Loraud, J.C., (1988). A multiphase formulation for fire propagation in heterogeneous combustible media. *International Journal of Heat and Mass Transfer*, 41(6-7), 881-897.
- Mei, R., Yu, D., Shyy, W. and Luo, L.S. (2002). Force evaluation in the lattice Boltzmann method involving curved geometry. *Physical Review E*, 65(4), p.041203.
- Mell, W., Maranghides, A., McDermott, R. and Manzello, S.L. (2009). Numerical simulation and experiments of burning douglas fir trees. *Combustion and Flame*, 156(10), 2023-2041.
- Tanino, Y., and H. M. Nepf. (2008). Laboratory investigation of mean drag in a random array of rigid, emergent cylinders. *ASCE, J. Hydraul. Eng.*, 134(1), 34–41.
- Tritton D. (1959). Experiments on the flow past a circular cylinder at low Reynolds numbers. *Journal of Fluid Mechanics*, 6(4), 547-567.
- U.S. Forest Service. (n.d.). U.S. Forest Service. Retrieved June 26, 2018, from <https://www.fs.fed.us/managing-land/fire>
- Wang, J., Wang, M. and Li, Z. (2007). A lattice Boltzmann algorithm for fluid–solid conjugate heat transfer. *International journal of thermal sciences*, 46(3), 228-234.
- Zhou, X., Mahalingam, S. and Weise, D. (2007). *Proceedings of the Combustion Institute*. Experimental study and large eddy simulation of effect of terrain slope on marginal burning in shrub fuel beds, 31(2), 2547-2555.
- Zou, Q. and He, X. (1997). Pressure and velocity boundary conditions for the lattice Boltzmann. *J. Phys. Fluids*, 9, 1591-1598.